Scientific Research Publishing

Journal of Materials Science and Chemical Engineering, 2024, 12, 83-93
https://www.scirp.org/journal/msce
ISSN Online: 2327-6053
ISSN Print: 2327-6045

Study on the Effect of Operating Parameters on Water Yield of Hollow Fibre Vacuum Membrane Distillation Using CFD Simulation and Response Surface Methodology

Xingtian Wang[1], Junfeng Zhu[1], Yingjie Wu[1], Junkui Niu[1], Danping Wang[2], Shiwen Hou[1]

[1]Institute of Pastoral Hydraulic Research, MWR, Hohhot, China
[2]Hohhot Meteorological Bureau, Hohhot, China
Email: mansub2007@163.com

How to cite this paper: Wang, X.T., Zhu, J.F., Wu, Y.J., Niu, J.K., Wang, D.P. and Hou, S.W. (2024) Study on the Effect of Operating Parameters on Water Yield of Hollow Fibre Vacuum Membrane Distillation Using CFD Simulation and Response Surface Methodology. *Journal of Materials Science and Chemical Engineering*, **12**, 83-93.
https://doi.org/10.4236/msce.2024.1211005

Received: October 24, 2024
Accepted: November 25, 2024
Published: November 28, 2024

Abstract

Coal chemical bases in Northwest China are suffering from geographical water scarcity and a large amount of highly saline wastewater that needs to be treated during the production process, resulting in water and energy consumption becoming a key issue in the process of confined zero discharge. Membrane distillation is a thermally driven water treatment technology that can achieve higher water production efficiency and lower energy consumption by using hollow fibre membrane distillation in combination with a vacuum permeation side. In this study, CFD simulation calculations and response surface method analysis of hollow fibre membrane modules were carried out to further reveal the effects of different process operating parameters on water yield and the interactions between the operating parameters. It was found that the influence of the parameters on the membrane flux was as follows: feed inlet temperature > vacuum pressure ≈ feed inlet flow rate > feed inlet sanility, and the optimal operating parameters were predicted to be vacuum pressure of 38.88 kPa, feed solution temperature of 353.15 K, feed solution concentration of 4.13%, and inlet velocity of 0.60 m/s, which achieve membrane flux of 38.90 $kg \cdot m^{-2} \cdot h^{-1}$ according to the response surface method. This study provides more in-depth theoretical guidance for the application of hollow fibre vacuum membrane distillation technology in the treatment of coal chemical high salt wastewater.

Keywords

Vacuum Membrane, CFD, Hollow Fibre, Response Surface, Membrane Flux

1. Introduction

Membrane distillation is a thermally-driven technology for the treatment of highly saline water, which primarily utilises water molecules on the hot side (the side containing the higher-temperature liquid) to evaporate when heated, pass through hydrophobic or hydrophilic microporous membranes, and then condense into a liquid to be recovered on the cold side (the side with the lower temperature) [1]. Because the micropores of the membranes are very small in size, typically in the micron to nanometer range, they effectively prevent liquid molecules and solutes from passing through, allowing only water vapour to pass through. And membrane distillation technology can be powered by using low-level heat, such as solar energy and industrial waste heat [2]. Membrane distillation technology consists of several different modes of operation, where Direct Contact Membrane Distillation (DCMD) allows liquids on the hot and cold sides to come into direct contact with both sides of the membrane [3], Air Gap Membrane Distillation (AGMD) provides a small air gap between the two sides of the membrane to reduce the direct contact of the liquids on the hot and cold sides [4], and Vacuum Membrane Distillation (VMD) facilitates the transfer of water vapour by applying a vacuum on one side of the membrane, which reduces the number of heat conduction between the hot and cold sides, which reduces heat loss and improves thermal efficiency [5].

In recent years, vacuum membrane distillation technology has attracted a lot of attention, especially for the treatment of coal chemical high salt wastewater [6]-[8]. However, low permeate flux, membrane fouling, long-term stability, pore wetting, and high energy cost are the biggest barriers to realising the application of vacuum membrane distillation technology due to the current technology [9]. Among other things, membrane distillation efficiency is dependent on heat, momentum, and mass transfer in the three domains of the membrane, permeate, and feed channel; therefore, understanding the underlying mechanisms and how the transport mechanisms interact is critical to the study of these processes and important parameters [10]. Due to the complexity of these systems, the study of local variables within the system requires significant processing time and cost. Therefore, simulations using computational fluid dynamics (CFD) models to predict the effects of relevant important parameters on membrane fluxes are very effective tools [11].

In the present study, we combined experimental and theoretical computational modelling to predict the distillation performance of different operating parameters for VMD applications. A systematic study in an aqueous solution with a salinity of 30 - 60 g per kg of water was used. In this approach, we considered the hydrodynamic and thermal behaviour in the feed stream to accurately assess the mass transfer efficiency of hollow fibre membrane distillation modules. Finally, the response surface method was used to predict the VMD distillate recovery performance for different brine concentrations under different operating conditions. Our study showed that for a fixed feed inlet temperature and vacuum pressure,

maintaining the feed flow at a higher flow rate is an important parameter to improve the permeate flux. Numerical simulations show that vacuum hollow fibre membrane distillation designed in this study is a promising technology for the treatment of high saline water for coal chemical industry.

2. Model Development

The VMD system consists of hollow fibre module, heater, condenser, feed solution tank, vacuum pressure chamber (permeate tank), and vacuum pump. The flow chart of the VMD system is shown in Figure 1.

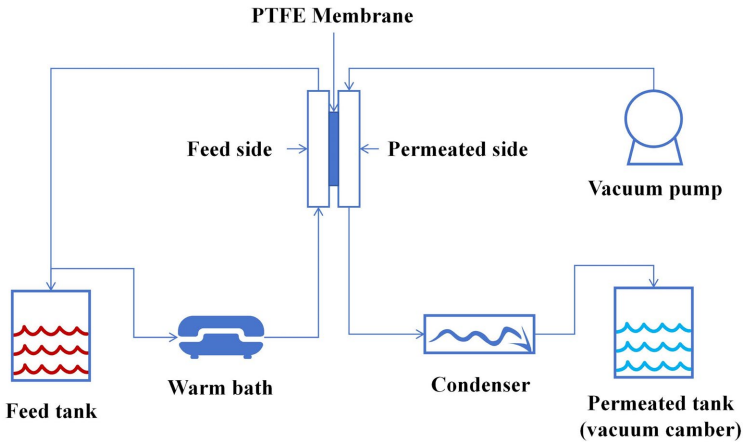

Figure 1. Flow chart of the VMD system.

Hollow fibre membranes were made of PTFE medium control fibre membranes with an average pore size of 0.16 μm and a porosity of 85% with an inner diameter of 0.8 mm and an outer diameter of 1.1 mm, the total number of membranes was 5 with a length of 400 mm. the overall dimensions of the VMD module were 8 mm (diameter) × 400 mm (length), and the model mesh design is shown in Figure 2. three different feed stream compositions were tested: salinity prepared with NaCl 30 g/kg, 45 g/kg and 60 g/kg of distilled water. The feed inlet temperature was 60˚C - 80˚C, the volumetric flow rate was 0.3 - 0.6 L/min, and the permeate vacuum pressure was varied between 10 - 90 kPa. The experimental conditions are summarised in Table 1.

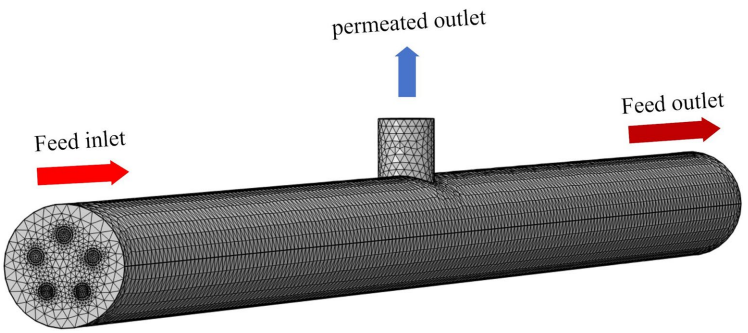

Figure 2. 3D geometry interpretation and meshing of membrane and its module test cell.

Table 1. Geometry specifications for model.

Hollow fiber membrane module	value
Effective length of fiber (mm)	400
Shell diameter (mm)	8
Amount of fibers	5
Inner diameter of fiber (mm)	0.8
Outer diameter of fiber (mm)	1.1
Porosity (%)	85
Mean pore diameter (μm)	0.16
Feed pressure (kPa)	350

3. Theoretical Modelling

3.1. Heat Transfer Model

During the VMD process, the permeate side region of the membrane is always in a high vacuum environment and the membrane material itself has poor thermal conductivity, so the heat loss is generally ignored in the modelling process According to the principle of energy conservation, the following equation can be obtained [12]:

$$Q_b = Q_m . \tag{1}$$

where Q_b is the heat of the feed liquid and Q_m is the latent heat of evaporation transfer.

The heat and latent heat of vapour transferred between the membrane surface and the feed liquid is calculated using the following equation [13]:

$$Q_b = h_f \left(T_f - T_{fm}\right) \tag{2}$$

$$Q_m = N\Delta H_V + \frac{K_m}{\delta}\left(T_{fm} - T_{pm}\right) \tag{3}$$

where δ is the membrane thickness (m), T_{fm} is the temperature of the membrane surface on the feed side (K), T_{pm} is the temperature of the membrane surface on the permeate side (K), N is the membrane flux per unit time ($kg{\cdot}m^{-2}{\cdot}h^{-1}$), and the equation of the relationship between the temperature of the membrane surface and the latent heat of vapour is as follows [14]:

$$\Delta H_V = 2489.7 - 2.412\left(T_{fm} - 278.15\right) \tag{4}$$

In the existing research literature, the calculation of heat transfer coefficients is based on the Nussell number. Although the models used in the various studies are different, the theory and procedure are basically the same. Based on these empirical formulas, the following Nussell's formula can be derived [15]:

$$N_u = \frac{h_f \cdot d}{k} \tag{5}$$

where d is the film thickness (m) and k is the thermal conductivity ($W \cdot m^{-1} \cdot K^{-1}$).

Local heat transfer coefficient on the material-liquid side [16]:

$$h_f = \frac{Q_b}{\left(T_f - T_{fm}\right)} = \frac{Q_m}{\left(T_f - T_{fm}\right)} \tag{6}$$

3.2. Mass Transfer Model

In membrane distillation operation, material transfer and heat transfer are interrelated processes. Thus, the membrane flux of VMD can be calculated by the following equation [17]:

$$H = K_m \cdot p = K_m \cdot \left(P_1 - P_2\right) \tag{7}$$

where P_1 is the membrane surface pressure (Pa) on the feed side and P_2 is the membrane surface pressure (Pa) on the permeate side.

On this basis, three main mass transfer mechanisms were proposed: molecular diffusion, Knudsen diffusion and viscous flow. In VMD, due to the negative pressure on the cold side, there is only a small amount of water vapour in the pore space of the membrane, and the resistance caused by the collision between molecules is negligible, and the driving force for the transfer is the saturated vapour pressure on the inlet side and the absolute pressure difference on the permeate side. The Knudsen number (K_n) is [17] [18]:

$$K_n = \frac{\lambda}{d} \tag{8}$$

where λ is the mean free range of water vapour (m) and d is the mean pore diameter of the membrane (m).

The calculated expression for the mean free range of water vapour through the membrane is as follows [19]:

$$\lambda = \frac{K_b T}{\sqrt{2}\pi P d_1^2} \tag{9}$$

where K_b has a value of 1.38×10^{-23} $J \cdot K^{-1}$ and d_1 is the collision diameter value of 2.641×10^{-10} m. The mass transfer mechanism in this study is a viscous flow-Nussen diffuser.

The mass transfer mechanism in this study is a viscous flow-Nussen diffusion machine, so the equation for the transmembrane mass transfer flux is [20]:

$$N = \left(C_1 + C_2\right)\Delta P \tag{10}$$

where C_1 is the viscous flow coefficient, C_2 is the Knudsen coefficient, and ΔP is the vapour partial pressure difference.

4. Membrane Flux Influences and Theoretical Predictions for VMD Systems

The membrane flux ($kg \cdot m^{-2} \cdot h^{-1}$) under different operating parameters was

obtained according to the simulation, and the interrelationships between feed inlet temperature, vacuum pressure, feed inlet flow rate and feed inlet sanility and membrane flux are shown in Figure 3, in which Figure 3(1) and Figure 3(4) show that the 3D response surfaces show irregular curvature, which indicates that there is an interplay between the feed inlet temperature and the vacuum pressure, and the feed inlet sanility and the vacuum pressure, and the membrane flux has a rapid and significant effect on the membrane flux with the increase of feed inlet sanility up to 6 g/kg. The increase of feed inlet sanility up to 6 g/kg has a rapid and significant effect on the membrane flux. Figure 3(5) shows the interaction between feed inlet flow rate and feed inlet temperature, and according to the image, it can be found that with the increase of feed inlet flow rate and feed inlet temperature, it has a significant effect on the increase of membrane flux. Whereas, Figure 3(2), Figure 3(3) and Figure 3(6) show the interactions between feed inlet sanility and vacuum pressure, feed inlet flow rate and vacuum pressure, and feed inlet flow rate and feed inlet sanility, respectively, and it can be seen that the above mentioned operating parameters have a relatively small effect on the membrane flux.

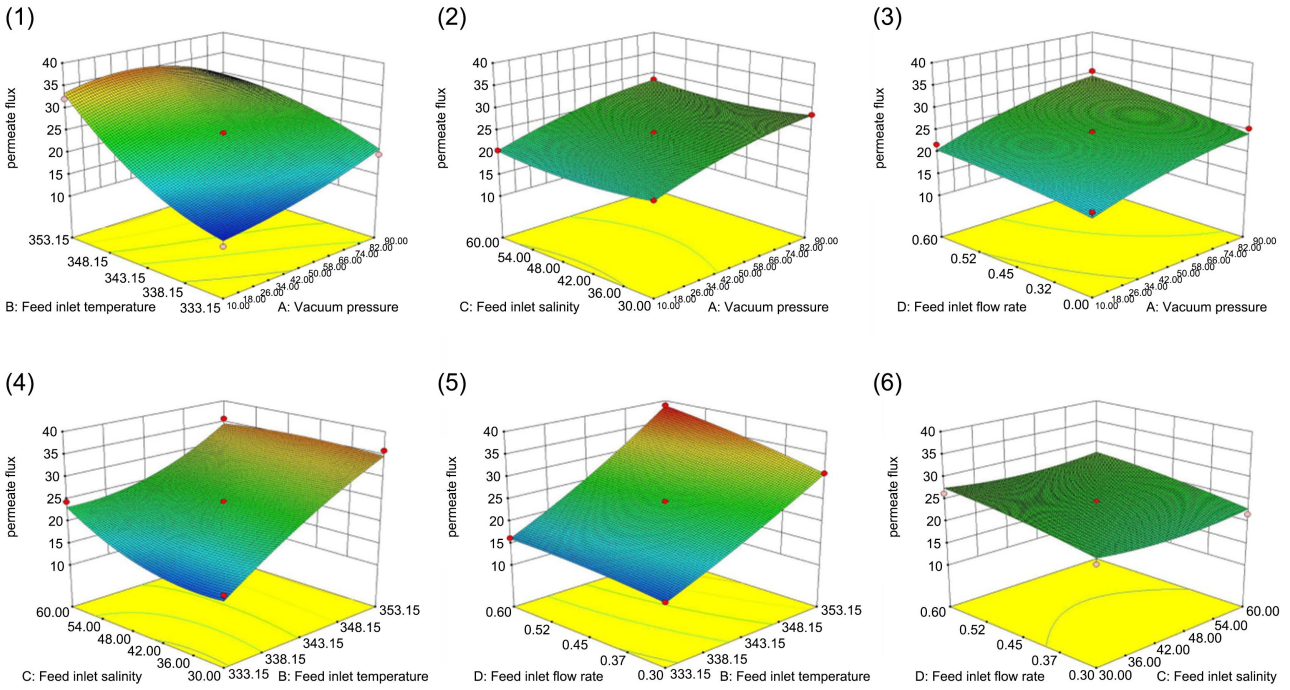

Figure 3. 3D response surface of operating parameters on membrane flux.

Figure 4 shows the contour plots of different operating parameters corresponding to the membrane flux. The figure reveals more clearly whether there are strong interactions between different operating parameters and the degree of influence on the membrane flux. In Figure 4(1), it can be seen that the influence of material temperature on membrane flux is significantly higher than that of vacuum pressure. Figure 4(2) shows that vacuum pressure has a stronger effect on membrane flux than feed solution concentration. In Figure 4(3), the effects of feed solution

inlet velocity and vacuum pressure on membrane flux are almost the same, and the interaction between these two influences is stronger, and together they play a key role in membrane flux. A stronger role of feed solution inlet temperature than concentration and feed solution inlet flow rate is also presented in Figure 4(4) and Figure 4(5). Figure 4(6) shows a stronger effect of feed inlet flow rate and a weaker correlation with feed inlet sanility. The corresponding membrane flux values for different operating parameters are shown in Table 2.

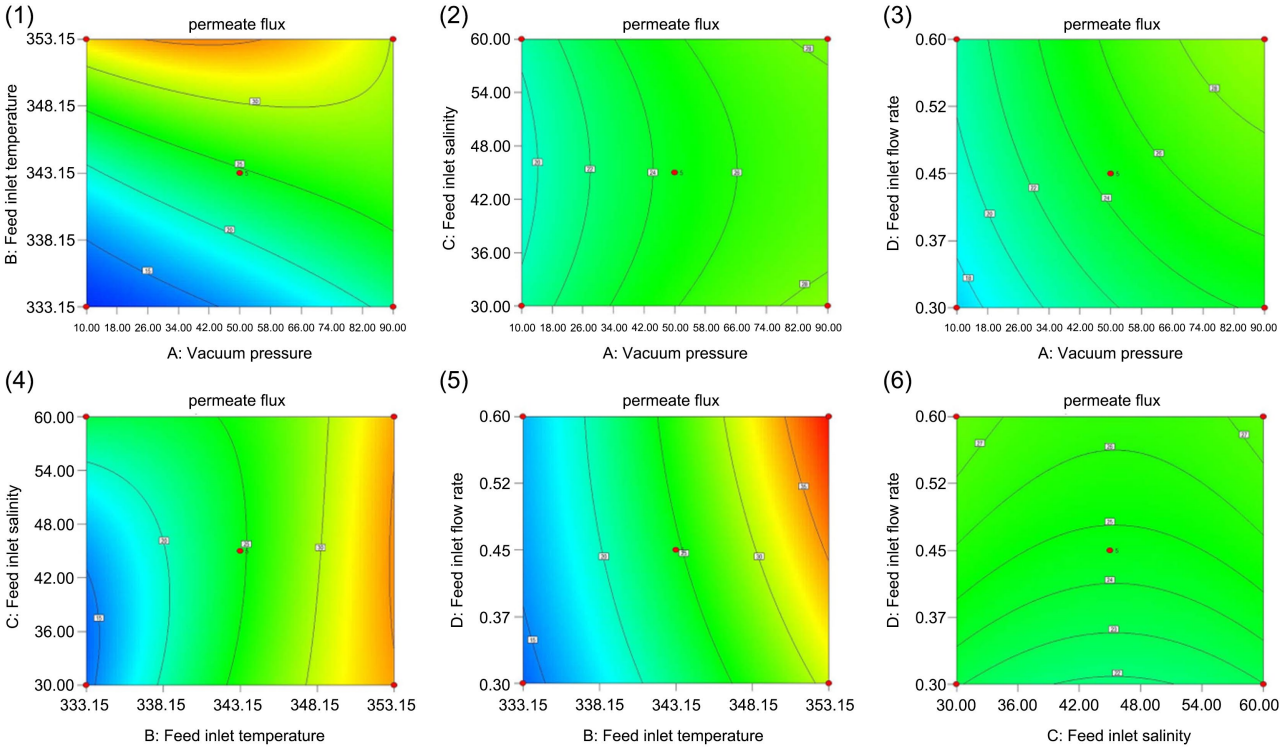

Figure 4. Contours of operating parameters on membrane flux.

Table 2. Membrane flux values are calculated from computational fluid dynamics simulations with different operating parameters.

vacuum pressure (kPa)	feed inlet temperature (K)	feed inlet salinity (g/kg)	feed inlet flow rate (m/s)	Permeate flux ($kg \cdot m^{-2} \cdot h^{-1}$)
10	343.15	30	0.45	20.76
50	333.15	30	0.45	15.47
50	343.15	30	0.3	21.84
50	343.15	30	0.6	26.4
50	353.15	30	0.45	35.87
90	343.15	30	0.45	28.63
10	333.15	45	0.45	11.2

Continued

10	343.15	45	0.3	18.21
10	343.15	45	0.6	21.8
10	353.15	45	0.45	32.15
50	333.15	45	0.6	16.24
50	333.15	45	0.3	13.99
50	343.15	45	0.45	24.59
50	343.15	45	0.45	24.59
50	343.15	45	0.45	24.59
50	343.15	45	0.45	24.59
50	343.15	45	0.45	24.59
50	353.15	45	0.6	38.9
50	353.15	45	0.3	30.91
90	333.15	45	0.45	19.67
90	343.15	45	0.6	30.48
90	343.15	45	0.3	25.44
90	353.15	45	0.45	28.56
10	343.15	60	0.45	20.59
50	333.15	60	0.45	24.51
50	343.15	60	0.3	21.71
50	343.15	60	0.6	26.22
50	353.15	60	0.45	35.67
90	343.15	60	0.45	28.48
10	343.15	30	0.45	20.76
50	333.15	30	0.45	15.47
50	343.15	30	0.3	21.84
50	343.15	30	0.6	26.4
50	353.15	30	0.45	35.87
90	343.15	30	0.45	28.63

According to the simulation calculation, the optimal operating parameters are vacuum pressure of 38.88 kPa, feed solution temperature of 353.15 K, feed solution concentration of 4.13%, and inlet velocity of 0.60 m/s, which can achieve the maximum membrane flux of hollow fibre vacuum membrane distillation module, which is 38.90 $kg \cdot m^{-2} \cdot h^{-1}$.

5. Conclusions

Computational fluid dynamics simulation calculations and response surface method were utilised to analyse the interactions under different operating parameters and according to the calculations, the degree of influence on the membrane flux was: feed inlet temperature > vacuum pressure ≈ feed inlet flow rate > feed inlet sanility. The optimal operating parameters were predicted to be vacuum pressure of 38.8 kPa, feed inlet temperature of 353.15 K, feed inlet sanility of 4.13%, and feed inlet flow rate of 0.60 m/s. In this study, computational fluid dynamics simulations were carried out from the tiny hollow fibre membrane distillation module to further analyse the influence of different operating parameters and the degree of influence on the change of membrane flux, which provided theoretical and technological support for the application of hollow fibre membrane distillation in the treatment of high saline wastewater. It provides theoretical and technical support for the application of hollow fibre membrane distillation in high salt wastewater treatment.

Acknowledgements

This work was supported by the Science and Technology Plan Program of Inner Mongolia Autonomous Region (2022YFHH0100) and Key special projects of the "Science and Technology for the Development of Inner Mongolia" initiative (2022EEDSKJXMO04).

Conflicts of Interest

The authors declare no conflicts of interest regarding the publication of this paper.

References

[1] Qasim, M., Samad, I.U., Darwish, N.A. and Hilal, N. (2021) Comprehensive Review of Membrane Design and Synthesis for Membrane Distillation. *Desalination*, **518**, Article 115168. https://doi.org/10.1016/j.desal.2021.115168

[2] Samadi, A., Ni, T., Fontananova, E., Tang, G., Shon, H. and Zhao, S. (2023) Engineering Antiwetting Hydrophobic Surfaces for Membrane Distillation: A Review. *Desalination*, **563**, Article 116722. https://doi.org/10.1016/j.desal.2023.116722

[3] Gulied, M., Zavahir, S., Elmakki, T., Park, H., Gago, G.H., Shon, H.K., *et al.* (2024) Efficient Lithium Recovery from Simulated Brine Using a Hybrid System: Direct Contact Membrane Distillation (DCMD) and Electrically Switched Ion Exchange (ESIX). *Desalination*, **572**, Article 117127. https://doi.org/10.1016/j.desal.2023.117127

[4] Lisboa, K.M., Curcino, I.V., Gómez, A.O.C., Chenche, L.E.P., Cotta, R.M. and Naveira-Cotta, C.P. (2024) A Reduced Model for Pilot-Scale Vacuum-Enhanced Air Gap Membrane Distillation (V-AGMD) Modules: Experimental Validation and Paths for Process Improvement. *Separation and Purification Technology*, **350**, Article 127891. https://doi.org/10.1016/j.seppur.2024.127891

[5] Pang, Z., Hou, C., Xie, S., Wong, N.H., Sunarso, J. and Peng, Y. (2022) Optimization of Hollow Fiber Membrane Module for Vacuum Membrane Distillation (VMD) via Experimental Study. *Desalination*, **542**, Article 116068.

https://doi.org/10.1016/j.desal.2022.116068

[6] Schnittger, J., McCutcheon, J.R., Hoyer, T., Weyd, M., Voigt, I. and Lerch, A. (2023) Modified Ceramic Membranes for the Treatment of Highly Saline Mixtures Utilized in Vacuum Membrane Distillation. *Desalination*, **567**, Article 116943. https://doi.org/10.1016/j.desal.2023.116943

[7] Murugesan, V., Rana, D., Matsuura, T. and Lan, C.Q. (2020) Optimization of Nanocomposite Membrane for Vacuum Membrane Distillation (VMD) Using Static and Continuous Flow Cells: Effect of Nanoparticles and Film Thickness. *Separation and Purification Technology*, **241**, Article 116685. https://doi.org/10.1016/j.seppur.2020.116685

[8] Zheng, L., Li, C., Zhang, C., Kang, S., Gao, R., Wang, J., *et al.* (2023) Mixed Scaling Deconstruction in Vacuum Membrane Distillation for Desulfurization Wastewater Treatment by a Cascade Strategy. *Water Research*, **238**, Article 120032. https://doi.org/10.1016/j.watres.2023.120032

[9] Bin Bandar, K., Alsubei, M.D., Aljlil, S.A., Bin Darwish, N. and Hilal, N. (2021) Membrane Distillation Process Application Using a Novel Ceramic Membrane for Brackish Water Desalination. *Desalination*, **500**, Article 114906. https://doi.org/10.1016/j.desal.2020.114906

[10] Zheng, L., Wu, Q., Ulbricht, M., Zhong, H., Duan, N., Van der Bruggen, B., *et al.* (2024) Contrasting Mixed Scaling Patterns and Mechanisms of Nanofiltration and Membrane Distillation. *Water Research*, **258**, Article 121671. https://doi.org/10.1016/j.watres.2024.121671

[11] Shirzadi, M., Li, Z., Yoshioka, T., Matsuyama, H., Fukasawa, T., Fukui, K., *et al.* (2022) CFD Model Development and Experimental Measurements for Ammonia-Water Separation Using a Vacuum Membrane Distillation Module. *Industrial & Engineering Chemistry Research*, **61**, 7381-7396. https://doi.org/10.1021/acs.iecr.2c00866

[12] Baghel, R., Kalla, S., Upadhyaya, S., Chaurasia, S.P. and Singh, K. (2020) CFD Modeling of Vacuum Membrane Distillation for Removal of Naphthol Blue Black Dye from Aqueous Solution Using COMSOL Multiphysics. *Chemical Engineering Research and Design*, **158**, 77-88. https://doi.org/10.1016/j.cherd.2020.03.016

[13] Xu, Z., Pan, Y. and Yu, Y. (2009) CFD Simulation on Membrane Distillation of NaCl Solution. *Frontiers of Chemical Engineering in China*, **3**, 293-297. https://doi.org/10.1007/s11705-009-0204-7

[14] Shakaib, M., Hasani, S.M.F., Ahmed, I. and Yunus, R.M. (2012) A CFD Study on the Effect of Spacer Orientation on Temperature Polarization in Membrane Distillation Modules. *Desalination*, **284**, 332-340. https://doi.org/10.1016/j.desal.2011.09.020

[15] Hasani, S.M.F., Sowayan, A.S. and Shakaib, M. (2019) The Effect of Spacer Orientations on Temperature Polarization in a Direct Contact Membrane Distillation Process Using 3-D CFD Modeling. *Arabian Journal for Science and Engineering*, **44**, 10269-10284. https://doi.org/10.1007/s13369-019-04089-x

[16] Shokrollahi, M., Rezakazemi, M. and Younas, M. (2020) Producing Water from Saline Streams Using Membrane Distillation: Modeling and Optimization Using CFD and Design Expert. *International Journal of Energy Research*, **44**, 8841-8853. https://doi.org/10.1002/er.5578

[17] Abrofarakh, M., Moghadam, H. and Abdulrahim, H.K. (2024) Investigation of Direct Contact Membrane Distillation (DCMD) Performance Using CFD and Machine Learning Approaches. *Chemosphere*, **357**, Article 141969. https://doi.org/10.1016/j.chemosphere.2024.141969

[18] Soukane, S., Naceur, M.W., Francis, L., Alsaadi, A. and Ghaffour, N. (2017) Effect of Feed Flow Pattern on the Distribution of Permeate Fluxes in Desalination by Direct Contact Membrane Distillation. *Desalination*, **418**, 43-59. https://doi.org/10.1016/j.desal.2017.05.028

[19] Zare, S. and Kargari, A. (2022) CFD Simulation and Optimization of an Energy-Efficient Direct Contact Membrane Distillation (DCMD) Desalination System. *Chemical Engineering Research and Design*, **188**, 655-667. https://doi.org/10.1016/j.cherd.2022.10.001

[20] Choi, J., Cho, J., Cha, H. and Song, K.G. (2024) Computational Fluid Dynamics Simulation of the Stacked Module in Air Gap Membrane Distillation for Enhanced Permeate Flux and Energy Efficiency. *Applied Energy*, **360**, Article 122805. https://doi.org/10.1016/j.apenergy.2024.122805